www.czasopisma.pan.pl PAN www.journals.pan.pl

ARCHIVES of FOUNDRY ENGINEERING

ISSN (2299-2944)
Volume 2020
Issue 3/2020

105 – 111

10.24425/afe.2020.133338

18/3

Published quarterly as the organ of the Foundry Commission of the Polish Academy of Sciences

Solid Particle Erosion of Laser Surface Melted Ductile Cast Iron

A. Kotarska *, D. Janicki, J. Górka, T. Poloczek
Silesian University of Technology, Department of Welding,
18A Konarskiego Str. 44-100 Gliwice, Poland
* Corresponding author. E-mail address: aleksandra.kotarska@polsl.pl

Received 23.12.2019; accepted in revised form 03.06.2020

Abstract

The article presents research on solid particle erosive wear resistance of ductile cast iron after laser surface melting. This surface treatment technology enables improvement of wear resistance of ductile cast iron surface. For the test ductile cast iron EN GJS-350-22 surface was processed by high power diode laser HPDL Rofin Sinar DL020. For the research single pass and multi pass laser melted surface layers were made. The macrostructure and microstructure of multi pass surface layers were analysed. The Vickers microhardness tests were proceeded for single pass and multi pass surface layers. The solid particle erosive test according to standard ASTM G76 – 04 with 30°, 60° and 90° impact angle was made for each multi pass surface layer. As a reference material in erosive test, base material EN GJS-350-22 was used. After the erosive test, worn surfaces observations were carried out on the Scanning Electron Microscope. Laser surface melting process of tested ductile cast iron resulted in maximum 3.7 times hardness increase caused by microstructure change. This caused the increase of erosive resistance in comparison to the base material.

Keywords: Ductile Cast iron, Laser surface melting, Erosion

1. Introduction

Erosion is the type of surface wear that is caused by the mechanical impact of solid or liquid particles. The mechanism of erosive wear and also the size of damage depends on many factors which include the type of abrasive particles (material, shape, size and mass), the impact angle (0 - 90°) or impact velocity. It was tested that the biggest damage of soft materials occurs when the impact angle is 20 - 30°, and for hard materials when the angle is about 90°. Because of these differences, the problem of erosive wear is complex. Erosive wear occurs in a variety of different industries, in machinery, and can cause significant financial losses. For these reasons, it is justified to protect surfaces that are exposed to erosion to decrease damage and financial loss caused by replacement or repair of machines components [1-4].

One of the popular materials used in many different applications in machinery is ductile cast iron because of its high mechanical strength and high plastic properties, low tendency to concentrate stress, very good casting properties, and machinability. However the wear resistance of this material is low, so for some applications were erosion, abrasion or other wear is occurring, ductile cast iron does not meet the requirements [5-9]. The way of protection against wear is the use of surface engineering technology at the production stage to increase surface hardness and, at the same time, wear resistance. Laser surface engineering is a group of surface engineering technologies that have high potential in use for many different materials with high precision. Because of the variation of laser surface technologies (e.g. hardening LTH, melting LSM, alloying LSA, cladding LC), production of surface layers with different structures and properties is possible. Therefore it is possible to design surface layer with specific properties (e.g. high wear resistance, corrosion resistance or hardness) using one of these methods. That is why laser surface modification is widely used in various applications for different materials [10-12]. Ductile cast iron can be processed

with each of laser surface modification technologies. In the literature, there is a wide range of researches about laser surface melting [13-18], alloying [19-23] and cladding [24-27] technologies of ductile cast iron for enhancing tribological properties. Laser surface melting process of ductile cast iron causes an improvement of surface hardness of up to 4 times [28]. This is a result of rapid cooling of liquid metal that occurs in this process. Hardness increase provides enhancement of wear resistance of the surface in comparison to the base material.

The aim of this research is to produce a surface layer on ductile cast iron substrate by laser surface melting process for wear resistance improvement. The study included macrostructure, microstructure observations, hardness measurements, solid particle erosive tests and worn surfaces observations on Scanning Electron Microscope.

2. Materials and methodology

For this research ductile cast iron (DCI) EN GJS-350-22 samples with dimensions 75 × 25 × 10 mm were used. The chemical composition of the material is presented in table 1. This cast iron has minimal tensile strength 350 MPa, minimal yield point 220 MPa and minimal elongation 22% [29]. The structure of ductile cast iron EN GJS-350-22 is ferritic (fig. 1) with spheroidal graphite with a diameter of about 65 µm and graphite area fraction about 20%.

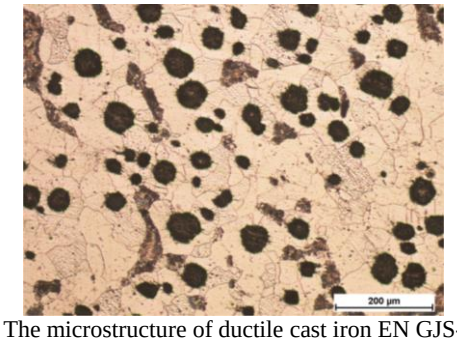

Fig. 1. The microstructure of ductile cast iron EN GJS-350-22

Table 1.
Chemical composition of ductile cast iron EN GJS-350-22

C	Si	Mn	P	S	Cu	Ti	Mg	Cr
3.66	2.71	0.527	0.042	0.001	0.068	0.032	0.012	0.124

Laser surface melting process was carried out on a test stand equipped with high power diode laser HPDL Rofin Sinar DL020 with direct beam emission on the surface and a numerically controlled positioning system of the head and the treated substrate. The laser beam used has a rectangular focus with dimensions of 6.8 × 1.8 mm with an even distribution of power density in the focus axis. During the process, the beam was focused on the surface of the material being processed. Argon with a flow rate of 20 l/min was used as the protective gas. For the tests single pass beads (SP) and multi pass surface layers (MP) were made. The erosive tests were carried out using multi pass surface layers with overlap 3.5 mm on 75 × 25 mm specimen surface. Parameters are presented in table 2. Produced surface layers were ground before tests.

Table 2.
Parameters of laser surface melting process

Surface layer number	Laser beam power, W	Laser melting speed, m/min
1	2000	0.2
2	2000	0.4
3	1500	0.075

The hardness of laser melted surface layers was measured using Vickers method with 200 g load on the cross-section of each single pass bead and multi pass surface according to the scheme (fig. 2). To receive average hardness and its standard deviation of each single pass bead surface layer, 10 additional measurements in this area were also made.

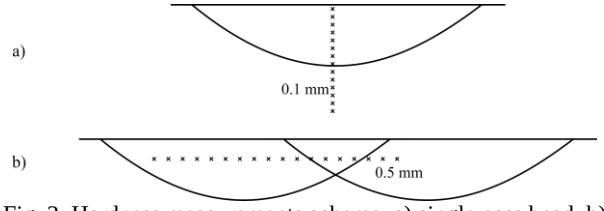

Fig. 2. Hardness measurements scheme, a) single pass bead, b) multi pass layer

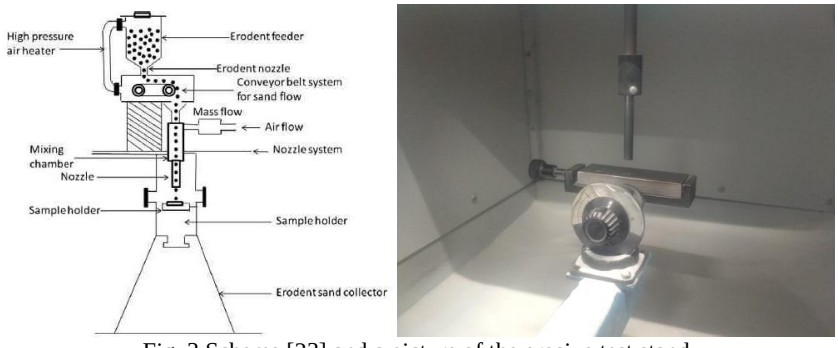

Fig. 3 Scheme [23] and a picture of the erosive test stand

Erosive wear test was carried out according to standard ASTM G76 – 04 [30]. The test stand is presented in figure 3. For the test Al_2O_3, 50µm diameter, abrasive particles in dry air were used as erodent. The velocity of abrasive particles was 70 m/s and its feed rate was 2 g/min. The test was carried out for 10 minutes for surface layers 1, 3 and reference material. Surface layer number 2 was tested for 8 minutes due to the lowest fusion depth of the surface layer. The tested sample surface was located in a distance of 10 mm to the nozzle. The test was carried out for each sample with the impact angle 90°, 60° and 30°. For each angle, 3 tests were carried out. As a result of solid particle erosive test, mass loss was obtained using laboratory-scale with an accuracy of 0.0001 g. The erosion rate and erosion value were counted for each sample using ASTM G76 – 04 standard [28]. Erosion rate is mass loss divided by total test time and erosion value is volume loss divided by the total mass of abrasive particles used in the test. The unit of erosion value is .001 mm^3/g. For observation of worn surfaces after erosive test Scanning Electron Microscope Phenom World PRO was used.

3. Results and discussion

Macrostructure of the laser melted multi pass, overlapping surface layer nr 1 is presented in figure 4. Cracks in this structure as a result of stresses occurring during subsequent melting cycles in the brittle surface layer can be observed. For each sample, the fusion depth was measured. The results are: first surface layer: 0.93 mm, second surface layer: 0.58 mm, third surface layer: 1.38 mm. Microstructure of laser melted surface layers shows figure 5. On figure 5a microstructure of laser melted zone is presented. Figure 5b shows the microstructure of heat-affected zone between subsequent beads of MP layer. Laser surface melting process on ductile cast iron substrate caused the microstructure change comparing to the as received DCI. During surface melting process graphite dissolved in liquid metal what caused increased carbon concentration in the liquid. As a result of the high cooling rate of liquid metal, that occurs in laser surface treatment, carbon precipitated in a form of cementite in surface layers. After this process, a very fine-grained structure consisted of primary austenite dendrites, partly after martensitic transformation and eutectic austenite and cementite in interdendritic spaces, was formed in surface layers.

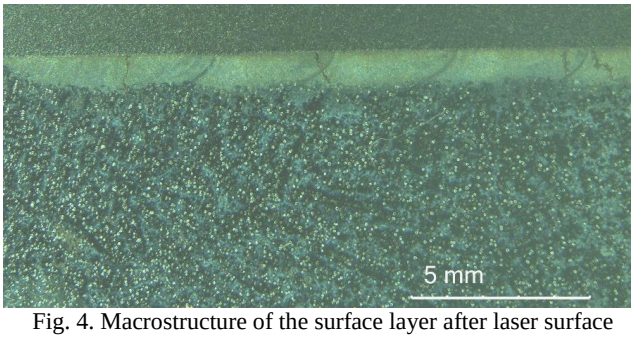

Fig. 4. Macrostructure of the surface layer after laser surface melting on EN GJS-350-22 ductile cast iron

Due to successive heating and melting in overlapping region of MP surface layers, change of structure in this area can be observed. The microstructure of heat-affected zone (HAZ) between subsequent beads consists of fine graphite spheroids in fine martensite and austenite matrix. During subsequent laser melting of the bead, cementite dissolved in liquid metal and due to different solidification conditions, carbon precipitated in heat-affected zone in a form of fine graphite.

Vickers hardness results are presented in figure 6. The average hardness of DCI EN GJS-350-22 is about 236 HV0.2. The single pass laser melting process has a positive impact on increasing hardness in comparison to as received DCI. The highest average hardness (875 HV0.2) out of all single pass surface layers was received for parameters 2000 W laser beam power and 0.2 m/min processing speed (surface layer nr 1) and the lowest for parameters 1500 W laser beam power and 0.075 m/min processing speed (surface layer nr 3). Analysing the hardness change on the cross-section graphs of SP layers (fig. 6b), it can be noticed that the hardness in the surface layer area is uniform and it decreases rapidly in the heat-affected zone. The average hardness of MP laser melted surface layers in comparison to SP samples decreased due to structural changes caused by subsequent heating and melting. The highest decrease for approximately 185 HV0.2 was noted for surface layer nr 1 (2000 W, 0.2 m/min). Average hardness of MP layer nr 3 (1500 W, 0.075 m/min) decreased for approximately 146 HV0.2 in comparison to SP laser melting and for surface layer nr 2 (2000 W, 0.4 m/min) occurred decrease for about 72 HV0.2. On the cross-section (fig. 6c) of MP laser melted surface layers hardness is uniform in laser melted region and decreases in HAZ.

In order to count resistance to erosion due to the standard ASTM G76 – 04 density of both, base material and the surface layer was tested using laboratory scales (Archimedes method). Base material density is 7.15 g/cm^3, the laser surface melted structure density is 7.39 g/cm^3. Erosion test results of laser surface melted layers and the reference sample which was ductile cast iron EN-GJS 350-22 are presented in table 3 and on figure 7. Figure 8 presents photos of worn surfaces after the erosive test, taken on a Scanning Electron Microscope.

Table 3.
Solid particle erosion test results

Impact angle	Sample number (tab. 2)	Average erosion value, $0.001mm^3/g$	Erosion value standard deviation, $0.001mm^3/g$
30°	1	46.91	3.47
	2	47.36	2.24
	3	49.79	3.05
	GJS 350-22	61.31	0.40
60°	1	37.89	3.77
	2	41.16	6.35
	3	36.08	1.56
	GJS 350-22	54.31	6.35
90°	1	38.34	6.43
	2	43.41	7.04
	3	39.24	2.44
	GJS 350-22	33.80	3.15

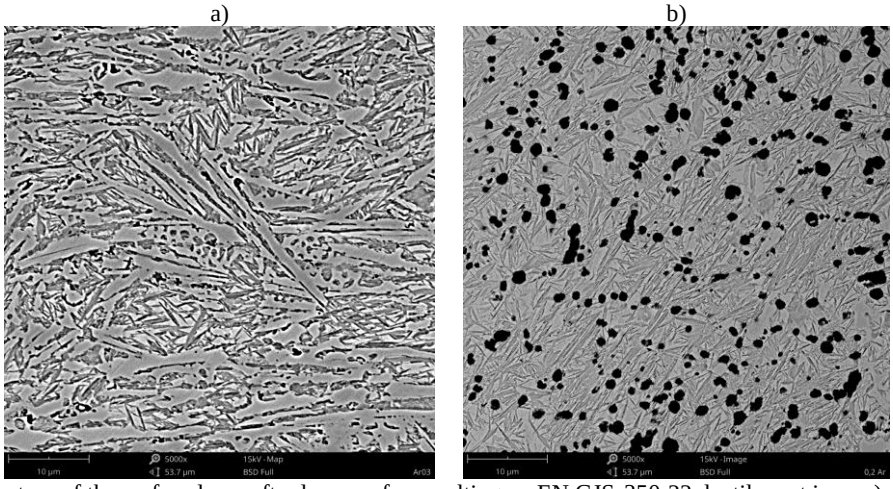

Fig. 5. The microstructure of the surface layer after laser surface melting on EN GJS-350-22 ductile cast iron, a) melted zone, b) heat-affected zone

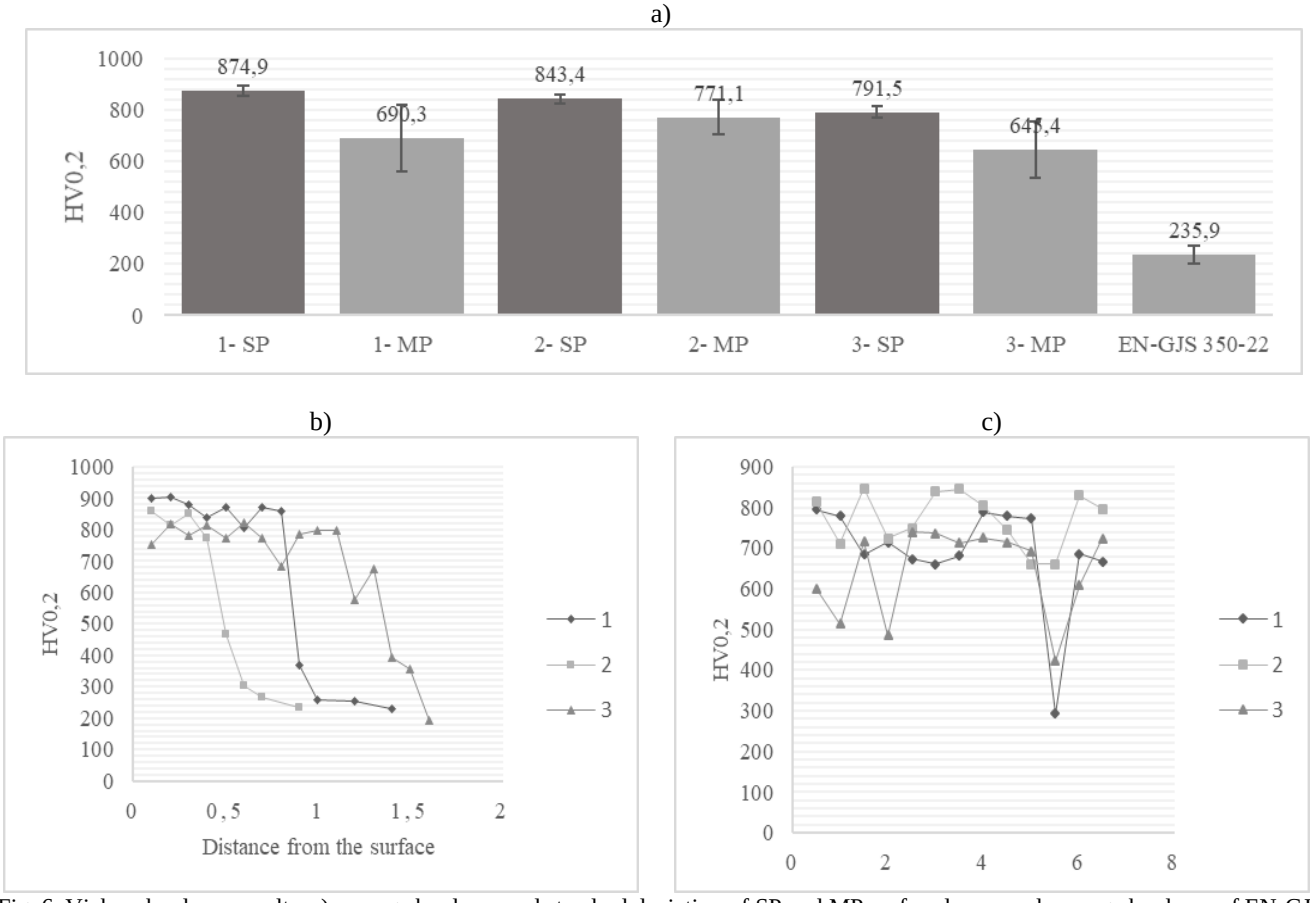

Fig. 6. Vickers hardness results, a) average hardness and standard deviation of SP and MP surface layers and average hardness of EN-GJS 350-22, b) graph of hardness change on the cross-section of the SP layers, c) graph of hardness change on the cross-section of the MP layers

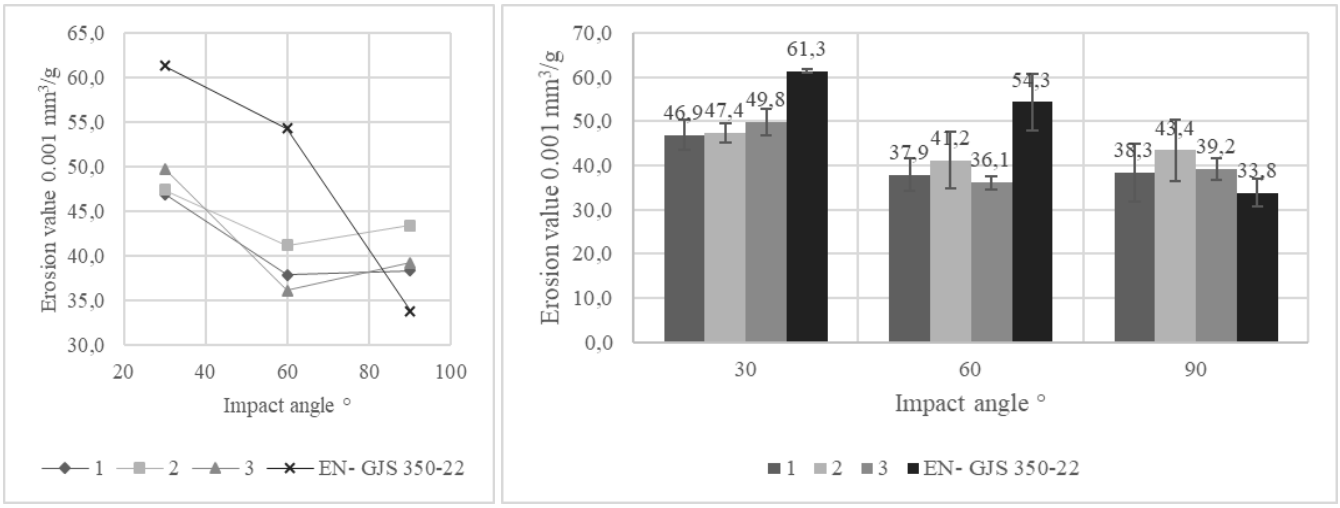

Fig. 7. Solid particle erosion test results

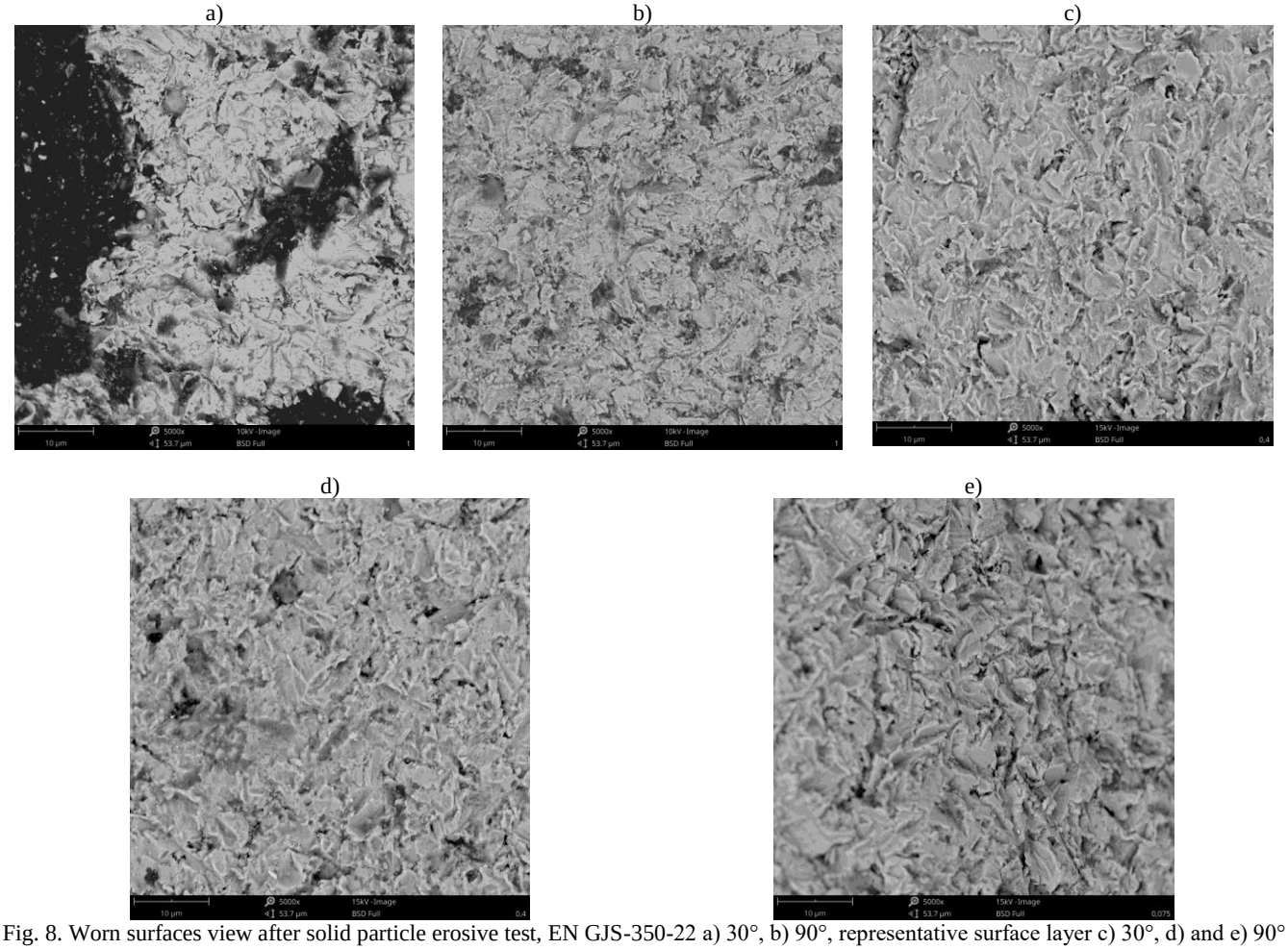

Fig. 8. Worn surfaces view after solid particle erosive test, EN GJS-350-22 a) 30°, b) 90°, representative surface layer c) 30°, d) and e) 90°

Average erosion value with impact angle 30° of all tested laser melted surface layers is similar and in comparison to the base material is lower for about 22%. In the tests carried out with impact angle 60° results for all surface layers are also similar and

in this conditions average erosion value decreased for about 30% comparing to base material. The tests carried out with the impact angle 90° ended with almost similar results for each sample, including reference base material EN-GJS 350-22. Due to the results, it can be concluded that laser surface melting process of ductile cast iron EN-GJS 350-22 increased the solid particle erosive wear resistance comparing to the base material, which is especially noticeable at lower impact angles (30° and 60°). It was tested that presence of cracks on laser melted surface layers affects decrease of erosive wear resistance for about 15%. In connection with such results, it should be stated that the occurrence of cracks in the structure of laser melted surface layers has a negative impact on their resistance to erosion.

SEM observations of worn surfaces after solid particle erosive test allowed to specify erosion mechanism of laser melted surface layers and reference material. Plastic deformation occurred on each of tested surfaces so erosive wear proceeded in a ductile mode. Due to the biggest differences, the analysis included craters obtained in tests with the impact angle of 30° and 90°. On the surfaces of ductile cast iron in contrast to laser melted surface layers, graphite areas can be observed. On the crater surfaces of laser melted layers tested with an impact angle of 30° (fig. 8c), wide and smooth scars can be seen together with narrow grooves. In case of tests carried out with an impact angle of 90° (fig. 8d), shallow craters can be observed on worn surfaces. On figure 8e is presented bigger plastic deformation of the HAZ between subsequent beads of MP surface layer. Higher wear that appeared in this region is caused by the change of the structure occurring as a result of succesive heating. In comparison to laser melted surface layers, plastic deformation on the reference material was more intensive. In case of surface tested with an impact angle of 90° (fig. 8b), deeper craters and bigger flakes can be seen on the worn surface. On the worn surfaces of the reference material tested with an impact angle of 30° (fig. 8a), deeper craters and grooves can be observed. On the craters of ductile cast iron and laser melted layers can be observed embedded Al_2O_3 erodent particles.

4. Conclusions

The laser surface melting of DCI results in producing surface layers with a fine-grained microstructure that consist of primary austenite dendrites, partly after martensitic transformation and eutectic austenite and cementite in interdendritic spaces. Heat-affected zone between subsequent beads of MP laser melted surface layer consists of fine graphite spheroids in martensite and austenite matrix. As a result of the microstructure change of DCI after single pass laser surface melting process, hardness was increased by 3.7 times. Multi pass laser surface melting with tested parameters and overlap 3.5 mm caused average hardness increase maximum 3.26 times comparing to as received DCI. The solid particle erosive test showed that laser surface melting process of ductile cast iron resulted in increasing erosive wear resistance by about 22% when the impact angle was 30°, and by about 30% when the impact angle was 60°. Tests carried out with impact angle 90° revealed similar results for tested surface layers and base material EN GJS-350-22. Due to the hardness decrease in heat-affected zone between subsequent beads of multi pass laser melted surface layers, erosive wear resistance decreases in this region. The presence of cracks has a negative impact on surface erosive wear resistance. It can be also concluded that surface hardness increase has a positive effect on increasing resistance to erosion.

References

[1] Stachowiak, G.W., Batchelor, A.W. (2014). *Engineering Tribology.* (4th ed.). Waltham: Butterworth-Heinemann.

[2] Shimizu, K., Noguchi, T., Seitoh, H., Okada, M. & Matsubara, Y. (2001). FEM analysis of erosive wear. *Wear.* 250, 779-784. DOI: 10.1016/S0043-1648(01)00716-5.

[3] Yaer, X., Shimizu, K., Matsumoto, H., Kitsufo, T. & Momono, T. (2008). Erosive wear characteristics of spheroidal carbides cast iron. *Wear.* 264, 947-957. DOI: 10.1016/j.wear.2007.07.002.

[4] Moravec, J., Novakova, I., at al. (2018). Application possibilities of the low-temperature repairs on creep-resistance turbine components from material GX23CrMoV12-1. *Innovative Technologies In Engineering Production (Itep'18.).* 244(01017), 1-8. DOI: 10.1051/matecconf/201824401017.

[5] Elliot, R. (1988). *Cast iron technology.* London: Butterworth & Co.

[6] Lerner, Y.S. (1994). Wear resistance of ductile irons. *Journal of Materials Engineering and Performance.* 3(3), 403-408. DOI: 10.1007/BF02645338.

[7] Żuk, M., Górka, J., Dojka, R. & Czupryński, A. (2017). Repair welding of cast iron coated electrodes. *IOP Conference Series; Materials Science and Engineering.* 277, 1-8. DOI:10.1088/1757-899X/227/1/012139.

[8] Petrus, Ł., Bulanowski, A., Kołakowski, J., Brzeżański, M., Urbanowicz, M., Sobieraj, J., Matuszkiewicz, G., Szwalbe, L. & Janerka, K. (2020). The influence of selected melting parameters on the physical and chemical properties of cast iron. *Archives of Foundry Engineering.* 17(1), 105-110.

[9] Jakubus, A. & Soiński, M.S. (2019). The influence of the shape of graphite precipitates on the cast iron abrasion resistance. *Archives of Foundry Engineering.* 14(4), 87-90.

[10] Kwok, C.T., Man, H.C., Cheng, F.T. & Lo, K.H. (2016). Developments in laser-based surface engineering processes: with particular reference to protection against cavitation erosion. *Surface & Coating Technology.* 291, 189-204. DOI: 10.1016/j.surfcoat.2016.02.019.

[11] More, S.R., Bhatt, D.V. & Menghani, J.V. (2017). Recent research status on laser cladding as erosion resistance technique – an overview. *Materials Today: Proceedings.* 4(9), 9902-9908. DOI: 10.1016/j.matpr.2017.06.291.

[12] Kwok, C.T. (2012). *Laser surface modification of alloy for corrosion and erosion resistance.* Cambridge: Woodhead Publishing Limited.

[13] Alabeedi, K.F., Abboud, J.H. & Benyounis, K.Y. (2009). Microstructure and erosion resistance enhancement of nodular cast iron by laser melting. *Wear.* 266, 925-933. DOI: 10.1016/j.wear.2008.12.015.

[14] Gadag, S.P. & Srinivasan, M.N. (1995). Cavitation erosion of laser-meted ductile iron. *Journal of Materials Processing*

Technology. 51, 15-163. DOI: 10.1016/0924-0136(94)01601-V.
[15] Pagano, N., Angelini, V., Ceschini, L. & Campana, G. (2016). Laser remelting for enhancing tribological performances of a ductile iron. *Procedia CIRP*. 41, 987-991. DOI: 10.1016/j.procir.2015.12.131.
[16] Janicki, D. (2018). *Shaping the structure and properties of surface layers of ductile cast iron by laser alloying.* Gliwice: Wydawnictwo Politechniki Śląskiej.
[17] Janicki, D. (2018). Microstructure and sliding wear behaviour of in-situ TiC-reinforced composite surface layers fabricated on ductile cast iron by laser alloying. *Materials.* 11, 1-17. DOI: 10.3390/ma11010075.
[18] Sun, G., Zhou, R., Li, P., Feng, A. & Zhang, Y. (2011). Laser surface alloying of C-B-W-Cr powders on nodular cast iron rolls. *Surface & Coatings Technology*. 205, 2747-2754. DOI: 10.1016/j.surfcoat.2010.10.032.
[19] Shamanian, M., Mousavi Abarghouie, S.M.R. & Mousavi Pour, S.R. (2010). Effects of surface alloying on microstructure and wear behaviour of ductile iron. *Materials and Design.* 31, 2760-2766. DOI: 10.1016/j.matdes.2010.01.017.
[20] Arabi Jeshvaghani, R., Shamanian, M. & Jaberzadeh, M. (2011). Enhancement of ductile iron surface alloyed by stellite 6. *Materials and Desing.* 32, 2028-2033. DOI: 10.1016/j.matdes.2010.11.060.
[21] Wróbel, T., Przyszlak, N. & Dulska, A. (2019). Technology of alloy layers on surface of castings. *International Journal of Metalcasting*. 13(3). 604-610. DOI: 10.1007/s40962-018-00304-x.
[22] Węgrzyn, T., Piwnik, J., Łazarz, B. & Tarasiuk, W. (2015). Mechanical properties of shaft surfacing with micro-jet cooling. *Mechanika (Kauno Technologijos Universitetas).* 21(5), 419-423. DOI: 10.5755/j01.mech.21.5.9545.
[23] Janerka, K, Jezierski, J., Bartocha, D. & Szajnar, J. (2014). Analysis of ductile iron production on steel scrap base. *International Journal of Cast Metals Research.* 27(4), 230-234. DOI: 10.1179/1743133614Y.0000000103.
[24] Winczek, J., Gucwa, M., Mičian, M., Koňar, R. & Parzych, S. (2019). The evaluation of the wear mechanism of high-carbon hardfacing layers. *Archives of Metallurgy and Materials*. 64(3), 1111-1115.
[25] Górka, J. (2002). Welding technologies for the removal of defects in welded joints and iron-castings. *Welding International.* 16(5), pp. 341-346. DOI: 10.1080/09507110209549543.
[26] Arias-Gonzalez, F., de Val, J., Comesana, R., Penide, J., Lusquinos, F., Quintero, F., Riveiro, A., Boutinguiza, M. & Pou, J. (2016). Fiber laser cladding of nickel-based alloy on cast iron. *Applied Surface Science*. 374, 197-205. DOI: 10.1016/j.apsusc.2015.11.023.
[27] Li, Y., Dong, S., Yan, S., Liu, X., He, P. & Xu, B. (2018). Surface remanufacturing of ductile cast iron by laser cladding Ni-Cu alloy coatings. *Surface & Coatings Technology*. 347, 20-28. DOI: 10.1016/j.surfcoat. 2018.04.065.
[28] Grum, J. & Sturm, R. (1996). Microstructure analysis of nodular iron 400-12 after laser surface melt hardening. *Materials Characterisation.* 37, 81-88. DOI: 10.1016/S1044-5803(96)00063-0.
[29] Standard: EN 1563:2018-10: Founding. Spheroidal graphite cast irons.
[30] Standard: ASTM G76 – 04: Standard test method for conducting erosion tests by solid particle impingement using gas jets.